Geophys. J. R. astr. Soc. (1978) **54**, 61–73

LISPB – V. Studies of crustal shear waves

M. Assumpção* *Institute of Geological Sciences, Murchison House, West Mains Road, Edinburgh EH9 3LA*

D. Bamford† *Department of Geophysics, University of Edinburgh, Mayfield Road, Edinburgh EH9 3JZ*

Received 1977 November 14; in original form 1977 September 23

Summary. Many shots in the LISPB profiles produced shear waves with large amplitudes which were recorded by three-component stations. However, *S* waves seem to be strongly attenuated when they propagate through complex velocity structures. Upper crustal refractions (mainly land shots) and wide-angle reflections (mainly sea shots) were picked with the help of particle motion plots. *S* to *P* travel-time ratios (t_s/t_p) were used to calculate the distribution of Poisson's ratios in a crustal model. The results were generally close to $\sigma = 0.25$ except in the upper crust south of the Southern Uplands Fault ($\sigma = 0.231$) and in the middle crust under the Midland Valley ($\sigma = 0.224$).

1 Introduction

A knowledge of the distribution of Poisson's ratio (or alternatively V_p/V_s) might be expected to add significantly to our understanding of the physical properties of, and processes in, the crust and upper mantle. However there is little published work on this subject presumably due to the difficulties of recording shear waves and picking their onsets accurately.

This paper describes the study of the *S* waves generated in some of the LISPB profiles (Bamford *et al.* 1976; Bamford *et al.* 1978), in particular on the segments ALPHA and BETA in Scotland (Fig. 1), and complements the determination of *P* wave velocity structure on segments ALPHA, BETA and GAMMA (Bamford *et al.* 1978). Conventionally Poisson's ratio (σ) is determined by the ratio of the apparent velocities of *P* and *S* waves at the surface with results usually in the range 0.23 to 0.27 but with large uncertainties of 0.01 or greater. The LISPB observations on closely spaced three-component stations allows σ to be determined with better accuracy than 0.01.

* On leave from University of São Paulo, Brazil.
† Present address: Geophysikalisches Institut, Universität, Karlsruhe, Germany.

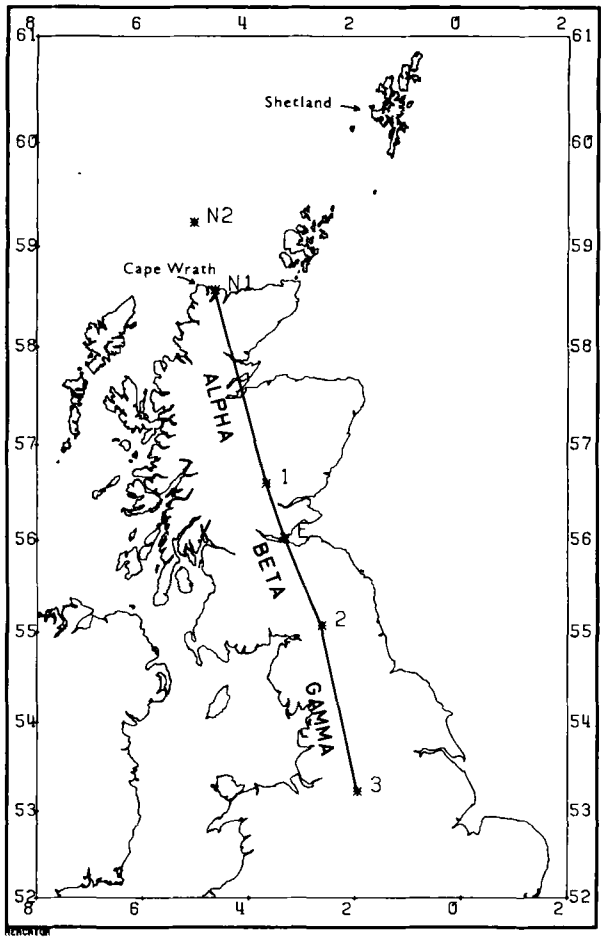

Figure 1. Location of shots and profiles.

2 Data quality

Not all of the LISPB shots generated good *S* waves but most shots recorded on ALPHA and BETA produced some shear waves either as upper crustal refractions (shots 1, E and 2; e.g. Fig. 2(a)) or as wide-angle reflections (shots N2, N1, 1 and E recorded on ALPHA, e.g. Fig. 2(b)).

The quality of *S* waves on segment GAMMA is far inferior to that on ALPHA and BETA and it seems that a relatively complex structure beneath GAMMA (Bamford *et al.* 1978) may be responsible. *S* waves may be easily attenuated by propagating through a structure with many velocity discontinuities. This could explain why land shot 2 (Fig. 2(a)) produced the best signal to noise ratio for *S* waves when recorded to the north (BETA) but no *S* waves when recorded to the south (GAMMA). Similarly, shot E produces reasonably clear *S* waves to the north (in the Midlands Valley and on ALPHA) to distances of 90 km whereas to the south the *S* waves are very poor, perhaps because of complex structure at and south of, the Southern Uplands Fault. In contrast, the absence of Moho reflections on both BETA and GAMMA may be due to the anomalous Moho transition identified by Bamford *et al.* (1978). No shear refractions from the Moho (conventionally called S_n) were detected on any of the crustal profiles.

The same notation has been adopted for *S* crustal phases as was used for *P* crustal phases by Bamford *et al.* (1978). Thus a_0 and a_1 are upper crustal refractions, e is a wide-angle reflection from the lower crust and c is the wide-angle Moho reflection.

3 *S* travel-time data

Record sections of those parts of the seismograms that might contain *S* were constructed with reduction velocity 3.464 km/s ($=6.0/\sqrt{3}$). For each shot there were three sections: one for the vertical, one for the radial horizontal and one for the transverse horizontal components (e.g. Fig. 2). A preliminary identification of *S* waves was made based on travel times using the *P* seismic sections as reference and assuming an average Poisson's ratio close to 0.25.

A time window of a few seconds and including the suspected *S* arrivals was then selected for each station for the plotting of particle motion diagrams: these diagrams show the ground motion in the sagittal plane (vertical-radial) and in the horizontal plane (radial-transverse). For this purpose the original records were filtered with a lowpass Hanning window, instead of a bandpass. This reduces the high-frequency background noise and at the same time does not diffuse the *S* onsets with the 'ringing' often caused by narrowband filters. The three components and the particle motions were then plotted and used for picking *S* arrivals, the vertical and radial components giving an *SV* onset and the transverse component an independent *SH* onset.

Not all stations had *S* waves with amplitudes large enough to be read. Out of 102 stations recording *P* arrivals for crustal refractions on profiles 1 – ALPHA, 1 – BETA, E – BETA + ALPHA, 2 – BETA, about 70 per cent produced *S* arrivals with a signal to noise ratio (SNR) large enough so that either *SV* or *SH* could be picked. Fig. 3 shows examples of *S* wave onsets of phase a_0 from profile 2 – BETA (for simplicity diagrams of particle motion in the horizontal plane were omitted).

It is known theoretically that the ground motion of *S* waves in a homogeneous half-space is not always linear but can be elliptical for shallow angles of emergence at the surface (e.g. Nuttli 1961; Meissner 1965). For example *SV* ground motion is elliptical for emergence angles (measured from the horizontal) less than 54.7 or 57.7° for Poisson's ratio 0.25 or 0.30 respectively. Non-linear *SV* ground motion was sometimes observed in the LISPB stations as illustrated in Fig. 3. More often the ground motion of the *S* wave train is more complicated than the examples in Fig. 3. The character of the *SV* and *SH* ground motion sometimes changes completely between adjacent stations, indicating that it is strongly affected by the structure very close to the surface (1 or 2 km beneath the station). For this reason no special processing could be applied to pick or enhance the *S* waves, like polarization filters (e.g. Montalbetti & Kanasewich 1970), where the same kind of ground motion would have to be assumed for all stations. Instead *SV* was picked with the help of particle motion plots as any motion with a phase difference between vertical and radial components ranging from 180° (linear motion) to ±90° (elliptical motion). The uncertainties in the *S* onsets varied approximately from $\pm T/4$ (good SNR) to $\pm T$ (poor SNR), where *T* is the main period of the *S* waves. Thus, land-shot arrivals for upper crustal phases (Fig. 2(a)) can have onsets accurate to about ±0.1 s or better whereas deeper penetrating arrivals for sea shots (Fig. 2(b)) can be determined to within ± 0.2 to ± 0.3 s.

4 Travel-time ratios (t_s/t_p)

For each station and for each phase, *S* travel times t_s were divided by the corresponding *P* travel time t_p and these ratios t_s/t_p were plotted against distance from the shot.

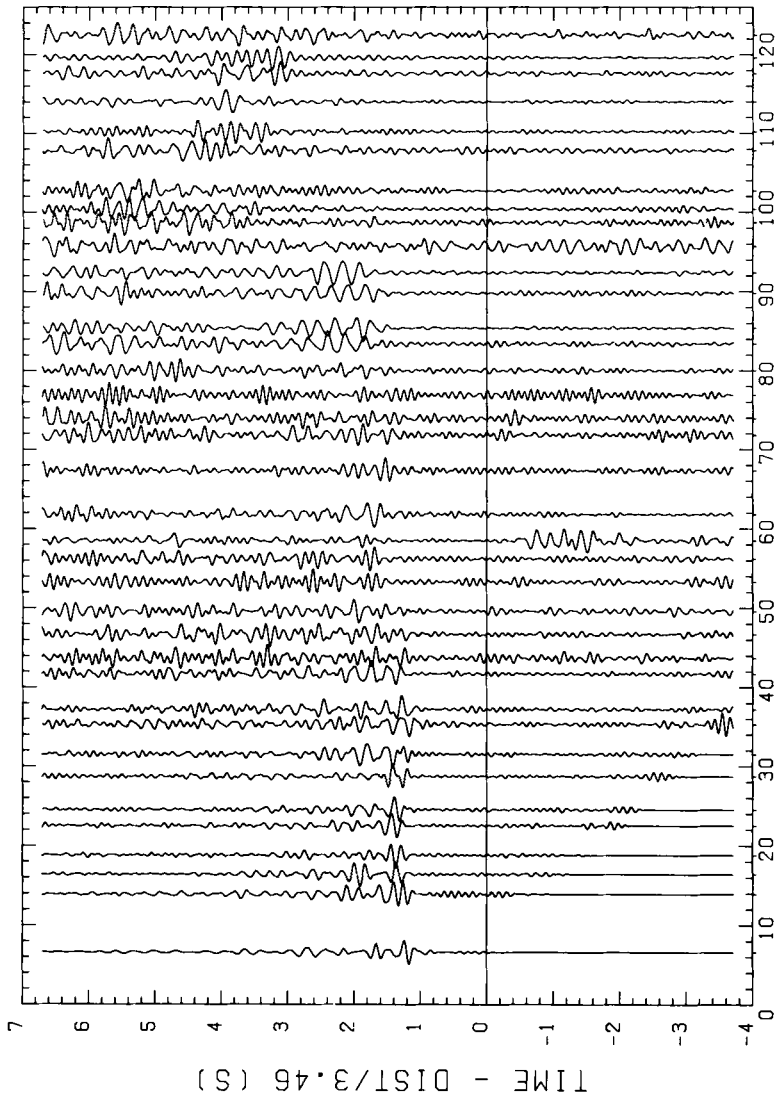

Figure 2 (a)

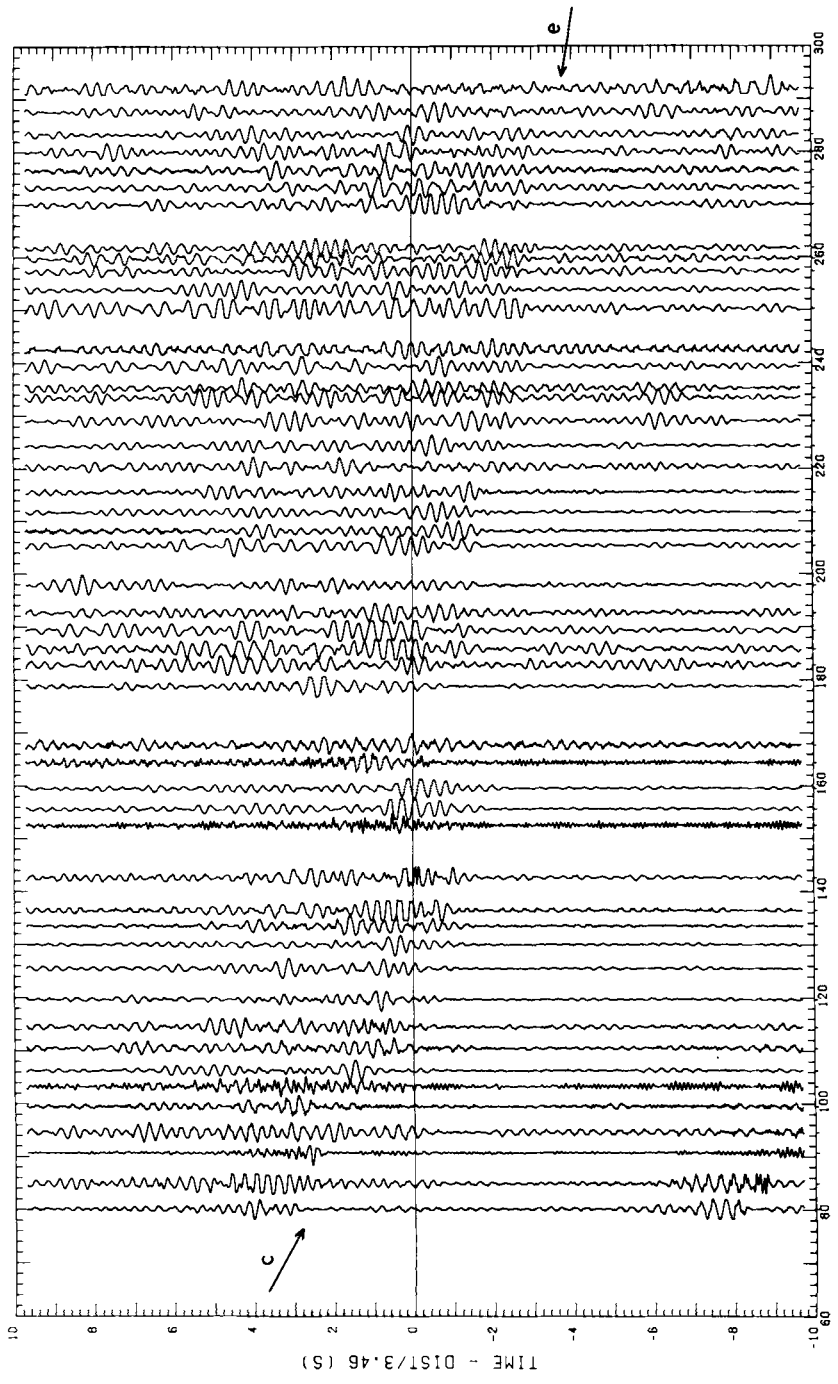

Figure 2 (b)

Figure 2. (a) Seismic section of shear waves, profile 2 – BETA (shot 2 recorded on segment BETA). Transverse component, bandpass filtered 2.5–10 Hz. The phase at about 1 s reduced time up to 100 km distance is a_0. (b) Seismic section of shear waves, profile N2 – ALPHA. Vertical component, unfiltered. Arrows indicate direction of phases c and e.

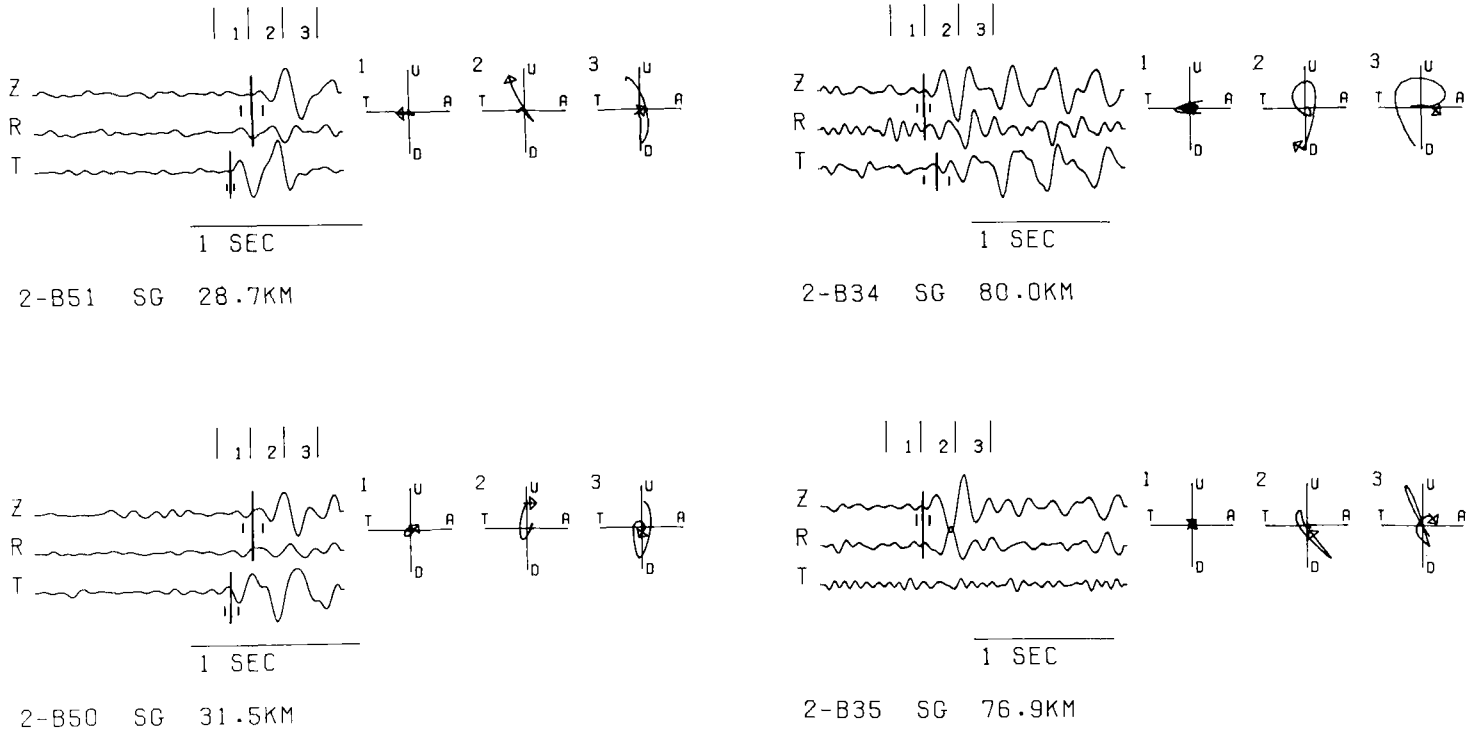

Figure 3. Examples of *S* arrivals and particle motion plots (*Z–R* plane). Phase a_0, profile 2 – BETA. The lines crossing the vertical and radial (*R*) components are *SV* picks, those crossing the transverse components (*T*) are *SH* picks. The two small lines on each side of the pick indicate its uncertainty. Particle motion diagrams refer to time windows marked on top of seismograms. U = up; D = down; T = towards the shot; A = away from the shot.

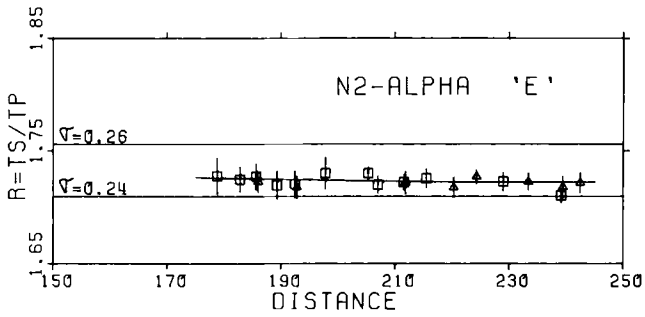

Figure 4. t_s/t_p travel-time ratio of phase e, profile N2 – ALPHA. The two horizontal lines were drawn at those values of t_s/t_p corresponding to $\sigma = 0.26$ and 0.24. The curve through the data is the theoretical curve from the model shown in Fig. 7. *SV* and *SH* data are indicated by squares and triangles respectively.

Fig. 4 shows a t_s/t_p plot for phase e from shot N2 (reflected from the bottom of layer 2, Fig. 7). The curve through the data points is the theoretical t_s/t_p curve given by the model to be explained below. Fig. 5 shows t_s/t_p plots for the upper crustal refractions (phase a_0 and a_1).

In the case of the crustal refractions, all shots have the same general trend of high t_s/t_p near the shot, decreasing with distance. This is explained by high values of σ near the surface, especially in sedimentary basins like the Midland Valley (Fig. 7, between HBF and SUF) and the Northumberland basin (Shot Point 2). Near the shot t_s/t_p is largely affected by the high σ of sediments, but as the waves travel longer distances in the refractor, below the sediments, the final t_s/t_p approaches the P to S velocity ratio of the refractor, which is lower than that of the sediments.

High values of σ in sediments, or generally near the surface, is the rule rather than the exception, as indicated by many field measurements like those of Jolly (1956); Erickson, Miller & Waters (1968); Geyer & Martner (1969); Tatham & Stoffa (1976) and Scarascia, Colombi & Cassinis (1976).

Laboratory measurements of Poisson's ratio in dry sandstones and limestones have a very wide range (e.g. King 1966; Gregory 1976) and are usually less than 0.25. However, rocks are usually porous and when specimens are filled with fluid, which is probably closer to the average condition in the field, then σ can increase significantly (King 1966; Gregory 1976). A small proportion of soft and unconsolidated sediments near the surface will also contribute to high average values of σ (Scarascia *et al.* 1976; Gregory 1976). So, Poisson's ratios as high as 0.33 near the surface as required by t_s/t_p data (see results below) are in general agreement with laboratory and field measurements.

5 Inversion of t_s/t_p ratios

It was not possible to use only the S wave data to get an independent model of S velocity structure, especially depths of boundaries, primarily because of the incompleteness of S refraction data and uncertainties in the S onsets. The following procedure was then used to calculate values of Poisson's ratios in a crustal model to fit all available t_s/t_p data.

The P velocity model suggested by Bamford *et al.* (1978) for Northern Britain was used as a reference. That model allows a small range of possible velocities in each layer. For the present purposes, we have used values from within the range which tend to be suggested by some additional modelling (especially ray-tracing) we have carried out. This reference model is shown in Fig. 6. One modification was made however under shot point 1 where the super-

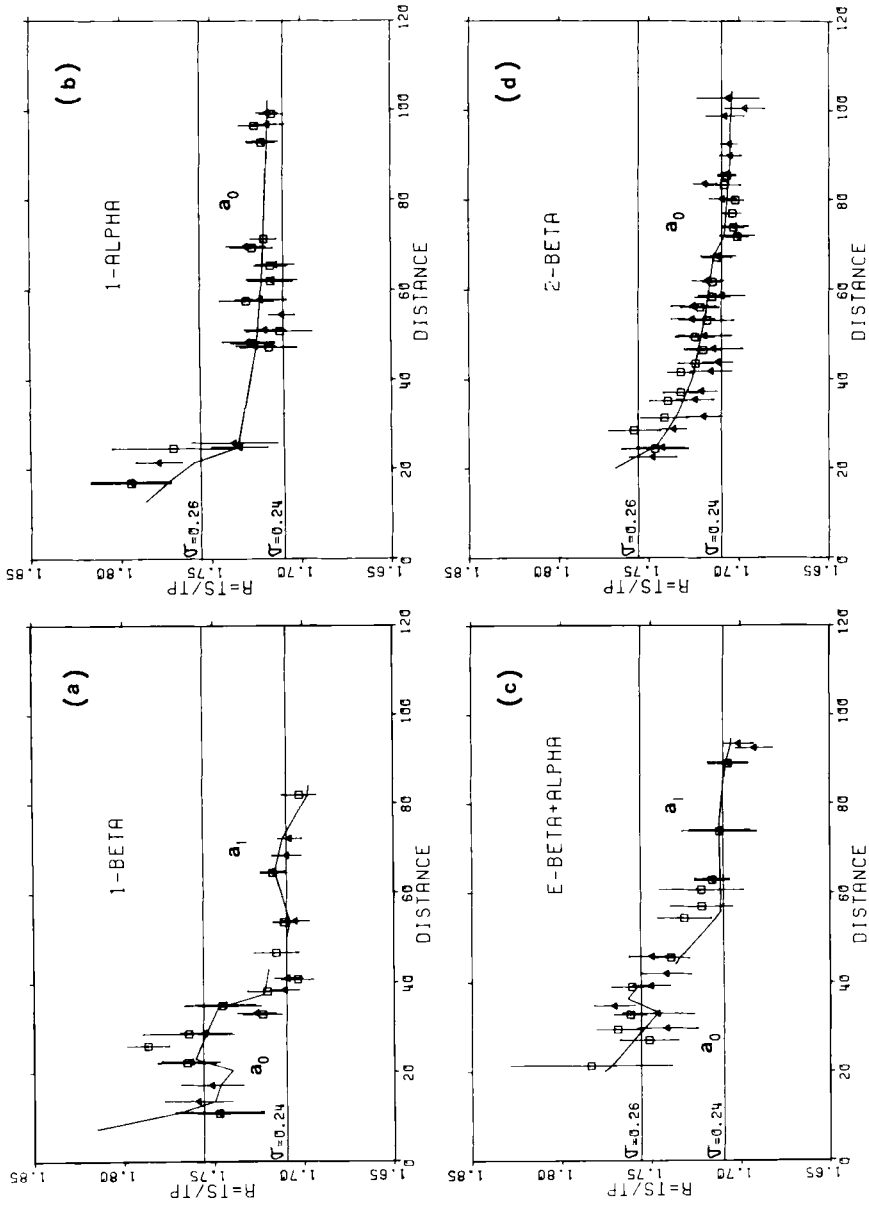

Figure 5. t_S/t_P travel-time ratios for crustal refractions. a_0 and a_1 refer to refractions through layers 1 and 2 respectively. Symbols as in Fig. 4.

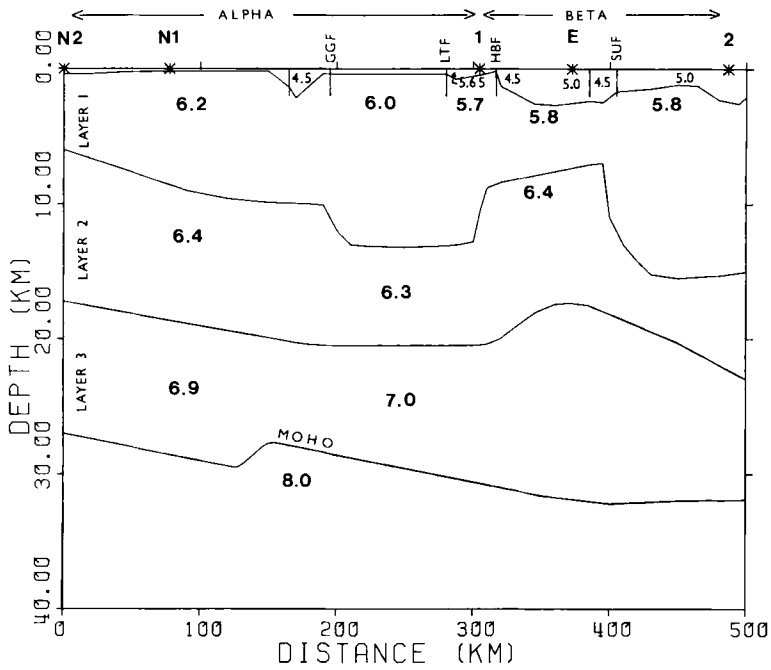

Figure 6. Reference crustal model for segments ALPHA and BETA (after Bamford *et al.* 1978) with *P* velocities in km/s. GGF, LTF, HBF, SUF, are Great Glen, Loch Tay, Highland Boundary and Southern Uplands Faults, respectively. Vertical exaggeration 10:1.

ficial layer of velocity 5.0 km/s and 0.2 km thickness was arbitrarily substituted by one dipping north with *P* velocity 5.65 km/s and thickness of 0.5 km (beneath shot 1). This is not in contradiction to the model of Bamford *et al.* because the scale of the LISPB experiment does not allow resolution of such details. Both models are equivalent in that they give about the same *P* travel times for stations near shot 1. Such a modification was found necessary in order to account for the t_s/t_p of stations within 15 km either side of shot 1.

The crustal layers were divided vertically into blocks with constant *P* velocities. The inversion of all t_s/t_p data to obtain Poisson's ratio σ in each block was done in two stages: (a) an initial model was found by a detailed trial and error search, and (b) the initial model was improved iteratively by a least-squares procedure. In the second stage the t_s/t_p functions were linearized with respect to their parameters σ by a Taylor-series expansion, and all profiles and phases (refractions + reflections) were used simultaneously in the inversion. Data from shots 1 and E, for example, had a reduced chi-square $\chi^2_\nu = 1.23$ (84 degrees of freedom) in the initial model; the solution of the first iteration had $\chi^2_\nu = 0.77$ and the process converged in the second iteration which gave results identical to the first.

Theoretical travel times for the t_s/t_p curves were calculated using an average horizontal-plane layer model allowing different layerings under the shot and under each station. Depths and *P* velocities were taken from the reference *P* velocity model.

The advantage of this method for calculating Poisson's ratios is that it is not critically dependent on an accurate *P* velocity model. Thus *P* velocities could be wrong by ± 0.1 km/s without affecting the theoretical t_s/t_p values at all. In this way, Poisson's ratios can be determined, particularly in the upper crust, with greater accuracy than by calculating *P* and *S* velocity independently and then forming the ratio of the two.

However, two assumptions have been made in order to determine Poisson's ratio structure. These are:

(i) That σ, as a first approximation, is constant with depth within each crustal block. This means that the σ value determined by a refraction which travels in the uppermost part of the refractor layer can be used as representative of the whole layer. For layer 1 under the Midland Valley (between shot points 1 and E) this is a reasonable assumption considering that σ is only slightly affected by changes in confining pressure and temperature for depths greater than about 4 km. For a change in confining pressure from about 1 kb (depth around 4 km) to 2 kb (depth around 8 km), σ usually increases by less than 0.005 (Simmons 1964; Christensen 1965, 1966). An increase in σ of 0.005 from the top to the bottom of layer 1 would produce an increase in t_s/t_p for refractions from layer 2 of only 0.001 in terms of Poisson's ratio, at distances around 50 km. Temperature has little effect on σ (Birch 1969) and a difference in temperature of the order of 40°C between depths of 4 and 8 km would produce a decrease in σ of less than 0.001, if Birch's results for olivine could be used only as an order of magnitude for upper crustal material. These values are much less than the measurement errors due to travel-time inaccuracies. On the other hand, between the Great Glen Fault and shot point 1 (Fig. 7) σ may not be constant throughout the whole depth of layer 1. From 2 km depth (probable depth of penetration of phase a_0) where pressure is about 0.5 kb down to 12 km where pressure is about 3 kb, Poisson's ratio could increase by as much as 0.010 (Simmons 1964; Christensen 1965, 1966).

(ii) That an average Poisson's ratio over a crustal block tens of kilometres long (or even more than a hundred kilometres long) is a good representation, as a first approximation, of the actual distribution of σ along the block. This hypothesis can only be tested by checking how well the theoretical t_s/t_p curves fit the observed data.

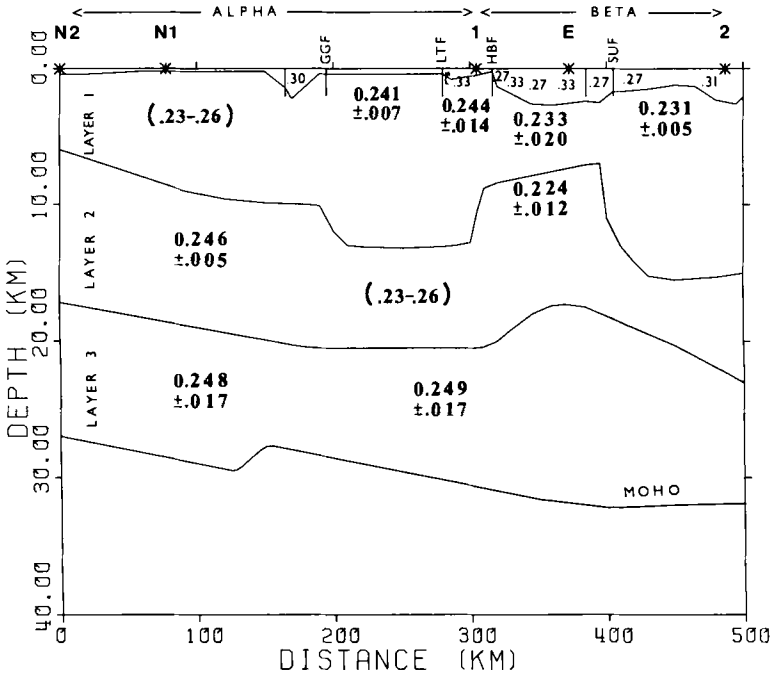

Figure 7. Poisson's ratio structure of segments ALPHA and BETA. Values in parenthesis are assumed range of σ. Uncertainties correspond to ± two standard deviations.

6 Results

Results of the Poisson's ratio modelling for segment BETA and ALPHA are shown in Fig. 7: the fits are reasonably good and some theoretical curves from the model are shown in Figs 4 and 5.

6.1 SEGMENT BETA

Shear wave sedimentary phases (distances less than about 10 km) did not have onsets sharp enough to define the average Poisson's ratio for the sediments with good resolution. Nevertheless these near-shot arrivals indicate that the average σ for the sedimentary layers lies roughly in the range 0.25 to 0.34. On the other hand in order to get a good fit to the t_s/t_p data for phase a_0, the sediments under shot points 1, E and 2 must have σ greater than 0.30. The various values of σ in the Midland Valley sedimentary layers between shots 1 and E (Fig. 7) were so chosen to account for relative high and low values of t_s/t_p on profiles 1 – BETA and E – BETA + ALPHA. For example $\sigma = 0.33$ to the south of the Highland Boundary Fault, Fig. 7, accounts for the relative high t_s/t_p of shot 1 – BETA at 22 km distance (Fig. 5(a)) and one from E – BETA + ALPHA at 46 km distance (Fig. 5(c)). The values of σ shown in the model of Fig. 7 for the sedimentary and superficial layers have then uncertainties around ± 0.03 and should be regarded as mere sedimentary corrections, or a kind of weathering correction in terms of Poisson's ratio. The important point is that this uncertainty of ± 0.03 does not significantly affect the determination of σ for the lower refractors a_0 and a_1. For example if under shot E, as shown in Fig. 7, σ was decreased by 0.03, σ for the a_0 refractor (layer 1) should be increased by only 0.007 to give the same t_s/t_p ratio at a distance of 40 km.

Although the overall fit for segment BETA is good, there is one misfit: phase a_0, 1 – BETA, near 40 km (Fig. 5(a) – theoretical curve too high) and phase a_1, E – BETA + ALPHA around 50 km (Fig. 5(c) – theoretical curve too low). It is difficult to improve the fit for shot 1 without worsening the fit for shot E. This suggests that a constant Poisson's ratio for layer 1 under the Midland Valley is not a very good approximation. Lower values of σ in the northern part and higher in the southern part (under shot point E) would probably correct that misfit. Nevertheless the data are not enough to justify the inclusion of one more parameter in the model and an average value of $\sigma = 0.233 \pm 0.020$ under the Midland Valley is retained.

No information is available for the bottom of the crust as deep reflections from this part of the profile were almost absent. This may be due in part, to the development of a relatively complex deep structure (Bamford *et al.* 1978).

6.2 SEGMENT ALPHA

For the northern part of ALPHA, no information about layer 1 is available as the *S* arrivals of shot N1 and N2 for phases a_0 and a_1 are too emergent. An assumed range of possible values from 0.23 to 0.26 was used for layer 1 in order to calculate σ for deeper layers.

In the southern part of ALPHA layer 1 has σ well determined by phase a_0 from shot 1 (at least in the upper part of layer 1, as explained before), but no information is available for layer 2. The same range of 0.23 to 0.26 for layer 2 was used to calculate σ for layer 3.

Poisson's ratio for layer 2 in the northern part of ALPHA is fairly well determined with phase e from shot N2 (reflection from the bottom of layer 2), Figs 2(b) and 4. In spite of the uncertainties in σ for the layer above it, σ for layer 2 was determined as 0.246 ± 0.005. This should be understood as an average of Poisson's ratio along layer 2 (say from a horizontal distance of 40 to 170 km). There is however, general agreement between this value and

one calculated from the ratio of apparent velocities determined by Smith & Bott (1975) for the same layer further north of the LISPB line, on a profile between Cape Wrath and Shetland. Their P and S velocities of 6.40 ± 0.09 and 3.76 ± 0.05 km/s respectively give $\sigma = 0.236 \pm 0.015$.

Poisson's ratios for the bottom of the crust have relatively larger uncertainties due to: (a) greater uncertainties in shear c onsets (compressional c can be picked to about ± 0.05 s after correlation processes are applied) and (b) uncertainties in σ of the upper layers, although in a smaller proportion, being transmitted to deeper layers.

7 Conclusion

The analysis of LISPB data demonstrates that explosions can be used in the study of shear waves and determination of crustal Poisson's ratios when three-component stations are employed. Although the signal to noise ratios of S waves from explosions are not usually as large as those from earthquakes, this deficiency is more than compensated for by the known origin time and high station density along a profile.

Difficulties in picking shear-wave arrivals are not only due to the fact that they are secondary arrivals (and so will always appear in a background of signal generated noise following the P waves), but also seem to be related to a more complicated type of ground motion (as compared to P waves) for shallow angle arrivals, depending strongly on the station site. Because of these difficulties S apparent velocities determined directly from the seismic sections have relatively large uncertainties. In contrast, use of the S to P travel-time ratio can sometimes allow the determination of Poisson's ratio with accuracies better than 0.01, as in layer 1 under the Southern Uplands and in layer 2 north of the Great Glen Fault.

LISPB Poisson's ratios were generally close to the conventional 0.25, except for layer 1 in the Southern Uplands ($\sigma = 0.231$) and layer 2 under the Midland Valley ($\sigma = 0.224$). These low values may indicate that these layers have anomalous physical properties possibly as a result of tectonic activity close to the Southern Uplands Fault. This would appear to confirm the region of the Southern Uplands Fault as a major point of interest in studies of Caledonian tectonics (Bamford *et al.* 1978).

Acknowledgments

This work was completed by MA as part of a PhD project at the University of Edinburgh with financial support from FAPESP, Brazil (Grant 74/627). We are greatly indebted to Dr P. L. Willmore for allowing full use of the facilities of the Global Seismology Unit of the Institute of Geological Sciences. We also thank Dr S. Crampin for helpful comments and assistance with the particle motion plotting programs.

References

Bamford, D., Faber, S., Jacob, B., Kaminski, W., Nunn, K., Prodehl, C., Fuchs, K., King, R. & Willmore, P., 1976. A lithosphere seismic profile in Britain – I. Preliminary results, *Geophys. J. R. astr. Soc.*, **44**, 145–160.

Bamford, D., Nunn, K., Prodehl, C. & Jacob, B., 1978. LISPB – IV. Crustal structure of Northern Britain, *Geophys. J. R. astr. Soc.*, **54**, 43–60.

Birch, F., 1969. Density and composition of the Upper Mantle: first approximation as an Olivine layer, in *The Earth's crust and upper mantle*, AGU monograph **13**, 18.

Christensen, N. I., 1965. Compressional wave velocities in metamorphic rocks at pressures to 10 kb, *J. geophys. Res.*, **70**, 6147–6164.

Christensen, N. I., 1966. Shear wave velocities in metamorphic rocks at pressures to 10 kb, *J. geophys. Res.*, **71**, 3549–3556.

Erickson, E. L., Miller, D. E. & Waters, K. H., 1968. Shear wave recordings using continuous signal methods, part II – later experiments, *Geophys.*, **33**, 240–254.

Geyer, R. L. & Martner, S. T., 1969. *SH* waves from explosive sources, *Geophys.*, **34**, 893–905.

Gregory, A. R., 1976. Fluid saturation effects on dynamic elastic properties of sedimentary rocks, *Geophys.*, **41**, 895–921.

Jolly, R. N., 1956. Investigation of shear waves, *Geophys.*, **21**, 905–938.

King, M. S., 1966. Wave velocity in rocks as a function of changes in overburden pressure and pore fluid saturants, *Geophys.*, **31**, 50–73.

Meissner, R., 1965. *P* and *SV*-waves from uphole shooting, *Geophys. Prosp.*, **13**, 433–459.

Montalbetti, J. F. & Kanasewich, E. R., 1970. Enhancement of teleseismic body phases with a polarization filter, *Geophys. J. R. astr. Soc.*, **21**, 119–129.

Nuttli, O., 1961. The effect of the Earth's surface on the *S* wave particle motion, *Bull. seism. Soc. Am.*, **51**, 237–246.

Scarascia, S., Colombi, B. & Cassinis, R., 1976. Some experiments on transverse waves, *Geophys. Prosp.*, **24**, 549–568.

Simmons, G., 1964. Velocity of shear waves in rocks to 10 kb, 1, *J. geophys. Res.*, **69**, 1123–1130.

Smith, P. J. & Bott, M. H. P., 1975. Structure of the crust beneath the Caledonian Foreland and Caledonian Belt of the North Scottish shelf region, *Geophys. J. R. astr. Soc.*, **40**, 187–205.

Tatham, R. H. & Stoffa, P. L., 1976. V_P/V_S – a potential hydrocarbon indicator, *Geophys.*, **41**, 837–849.